

Highly selective CD44-specific gold nanorods for photothermal ablation of tumorigenic subpopulations generated in MCF7 mammospheres

This article has been downloaded from IOPscience. Please scroll down to see the full text article.

2012 Nanotechnology 23 465101

(<http://iopscience.iop.org/0957-4484/23/46/465101>)

View [the table of contents for this issue](#), or go to the [journal homepage](#) for more

Download details:

IP Address: 165.132.140.220

The article was downloaded on 07/12/2012 at 05:42

Please note that [terms and conditions apply](#).

Highly selective CD44-specific gold nanorods for photothermal ablation of tumorigenic subpopulations generated in MCF7 mammospheres

Eugene Lee^{1,6}, Yoochan Hong^{2,6}, Jihye Choi³, Seungjoo Haam^{3,4},
Jin-Suck Suh^{1,4}, Yong-Min Huh^{1,4} and Jaemoon Yang^{1,4,5}

¹ Department of Radiology, College of Medicine, Yonsei University, Seoul 120-752, Korea

² Department of Biomedical Engineering, Yonsei University, Wonju, Gangwondo, 220-710, Korea

³ Department of Chemical and Biomolecular Engineering, Yonsei University, Seoul 120-749, Korea

⁴ YUHS-KRIBB Medical Convergence Research Institute, Seoul 120-752, Korea

⁵ Severance Integrative Research Institute for Cerebral & Cardiovascular Diseases, Yonsei University Health System, Seoul 120-752, Korea

E-mail: ymhuh@yuhs.ac and 177hum@yuhs.ac

Received 21 June 2012, in final form 14 September 2012

Published 23 October 2012

Online at stacks.iop.org/Nano/23/465101

Abstract

Heterogeneous stem-like populations within tumor tissues are the primary suspects in causing cancer recurrence and malignancy. It is essential to selectively kill these tumorigenic populations. We created a novel system for photothermally ablating specific cells from three-dimensional mammospheres. A CD44-positive subpopulation, with tumorigenic and self-renewal potential, spontaneously arises in MCF7 breast cancer cell-engineered mammospheres. Using anti-CD44 antibody-linked gold nanorods, which strongly absorb near infrared light and increase local temperature, we effectively targeted and photo-ablated atypical cells. This biomarker-specific photothermal ablation model, using a smart nanoplatform, is a promising new strategy for selectively killing cancer cells, while sparing normal tissues.

(Some figures may appear in colour only in the online journal)

1. Introduction

Cancer cells exhibit complex heterogeneity, using diverse oncogenic signaling mechanisms and metabolic pathways [1, 2]. Recent reports have shed light on the role of cancer stem cells, or tumor-initiating cells, in tumorigenicity and metastasis [3, 4]. Cancer stem cells, a subpopulation of cells within a tumor, are capable of self-renewal and generate heterogeneous cancer cell lineages [5]. These cells play pivotal roles in tumor initiation, invasion, metastasis, and drug resistance [6]. Furthermore, cancer stem cells may express cancer stem cell-specific antigens as molecular markers

and recent research has focused on the understanding of these molecular markers for signaling mechanisms related to the biology of cancer stem cells [7]. Thus, it is very important to selectively target and kill tumorigenic cell subpopulations (cancer stem cells) on the basis of specific molecular markers as potential targets for effective cancer therapy [8]. A promising therapeutic modality for cancer treatment is using tumor marker-directed light-absorbing gold nanoparticles [9–11]. After specific binding to target cells, exposure to near infrared (NIR) laser energy causes localized photothermal ablation of the target cells, while sparing surrounding normal tissues [12]. This selective targeting is a major benefit of this approach, as classical cancer

⁶ These authors contributed equally to this work.

treatments such as chemotherapy and radiotherapy have numerous detrimental systemic side effects [13]. Since solid tumors are comprised of a heterogeneous cell population, biomarker-specific targeting is an effective method for ablating cancer cells through photothermally heated gold nanoparticles [12, 14]. Recently, Al-Hajj *et al* reported that breast cancer neoplasms can be divided into tumorigenic and non-tumorigenic cellular subgroups on the basis of surface marker expression [6]. CD44 is a marker for identifying stem cell-like cancer cells. CD44 may be one of the most important adhesion molecules facilitating cancer cell invasion and metastasis [15, 16].

In this report, we demonstrate the specific targeting and destruction of tumorigenic CD44-positive cancer cells using selective plasmonic nanoparticle attachment to these cells, followed by NIR light irradiation to cause photothermal ablation. As a model system, mammospheres built using the MCF7 cell line have an apparent lumen and demonstrate increased tumorigenic populations [17]. The parent MCF7 cell line has an epithelial-like monolayer phenotype and lacks a CD44-positive subpopulation. However, Ao *et al* reported that MCF7 mammospheres exhibited high CD44 expression level and *in vivo* tumorigenic potential in contrast to their parental MCF7 cell monolayers [17]. Furthermore, Xie *et al* observed that MCF7 mammospheres contained CD44-positive cells and were more radio-resistant than cells grown in monolayers [18]. After carrying out growth in sphere-inducing culture conditions, therefore, we assessed tumorigenic CD44 expression in the MCF7 mammosphere model system, using flow cytometry and confocal microscopy. To prepare the marker-specific photothermal probes, plasmonic gold nanorods (GNRs) were synthesized by a seed-mediated growth method and polyethylene glycol-coated using a carboxylic thiol PEG for substitution of a cationic surface ligand [10]. Biocompatibility of PEG-coated GNRs (PGNRs) was evaluated by the MTT assay. For the targeted delivery of GNR to CD44-expressing cancer cells, we immobilized anti-CD44 antibodies on the carboxylated PGNR by carbodiimide chemistry [19]. Targeting of CD44-conjugated PGNRs to CD44-expressing MCF7 cell populations in mammospheres was investigated by reagent/cell co-incubation, followed by dark-field microscopy assessment. Furthermore, specific targeting and photothermal killing capabilities of CD44-conjugated PGNRs for CD44-expressing MCF7 cells in mammospheres were verified by a fluorescence live–dead assay and flow cytometry.

2. Materials and methods

2.1. Materials

Gold (III) chloride trihydrate ($\text{HAuCl}_4 \cdot 3\text{H}_2\text{O}$), hexadecyltrimethylammonium bromide (CTAB), sodium borohydride, silver nitrate, L-ascorbic acid, and 1-ethyl-3-(3-dimethylaminopropyl)-carbodiimide (commercial grade) were purchased from Sigma-Aldrich (St. Louis, MO). *N*-hydroxysulfosuccinimide was purchased from Pierce. Thiol-poly(ethylene glycol)-carboxymethyl (M_w : 3400 Da)

was purchased from Laysan Bio Inc. Anti-CD44 antibody as a targeting moiety was purchased from Cell Signaling Technology. Dulbecco's phosphate-buffered saline (PBS, pH 7.4) was purchased from Hyclone. All other chemicals and reagents were of analytical grade. Ultrapure deionized (DI) water was used for all of the synthesis processes.

2.2. Formation and characterization of MCF7 mammospheres

For mammosphere formation, MCF7 cells (5×10^5 cells/well) were seeded into ultra-low attachment-coated culture plates (100 mm diameter, Corning) in serum-free DMEM (Gibco) supplemented with 1% antibiotics (Gibco). Culture media were changed every two days.

The expression of CD44 and EpCAM on MCF7 mammospheres was determined by flow cytometry (FAC-Scalibur, Becton–Dickinson). Single-cell suspensions from mammospheres (1×10^6 cells) were collected, washed three times with blocking buffer 0.2% fetal bovine serum and 0.02% sodium azide in PBS (pH 7.4) to prevent non-specific binding of antibodies, and then incubated with 5 μl fluorescein isothiocyanate (FITC)-conjugated anti-mouse EpCAM (0.5 $\mu\text{g } \mu\text{l}^{-1}$, BD Biosciences) and 10 μl phycoerythrin (PE)-conjugated anti-human CD44 (BD Biosciences) for 30 min at 4 °C. Cells were resuspended in 400 μl 4% paraformaldehyde solution and stored at 4 °C prior to flow cytometry.

For confocal microscopy, MCF7 mammospheres (7 days) were incubated with (1:10) FITC-conjugated EpCAM and FITC-conjugated mouse anti-human CD44 (BD Biosciences) for 60 min at 4 °C. Nuclei were stained using Hoechst 33342 (BD Biosciences). CD44 and EpCAM expression levels on MCF7 mammospheres were observed using laser scanning confocal microscopy (LSM700, Carl Zeiss).

2.3. Preparation of gold nanorods (GNRs)

Monodispersed GNRs were prepared using a seed-mediated growth method as in a previously published protocol [10]. In brief, to prepare the gold–seed solution, 250 μl of $\text{HAuCl}_4 \cdot 3\text{H}_2\text{O}$ (10 mM) solution was added to 7.5 ml of hexadecyltrimethylammonium bromide (CTAB) (93 mM) solution and then 600 μl of ice-cold sodium borohydride (10 mM) was added to the mixture with vigorous stirring. The mixture was allowed to react for 2 min and stored at room temperature for 4 h. And then a growth solution was prepared as follows. The CTAB solution was prepared under vigorous stirring, and then 80 μl of silver nitrate (10 mM) solution, 500 μl of $\text{HAuCl}_4 \cdot 3\text{H}_2\text{O}$ (10 mM) solution, 55 μl of ascorbic acid (100 mM) solution and 12 μl of gold–seed solution were successively dropped into prepared CTAB solution and stirred for 30 s. The product solution was stored at room temperature for 24 h. The resultant solution was centrifuged three times at 15 000 rpm for 30 min to remove the excess CTAB molecules and re-dispersed in 5 ml of deionized water.

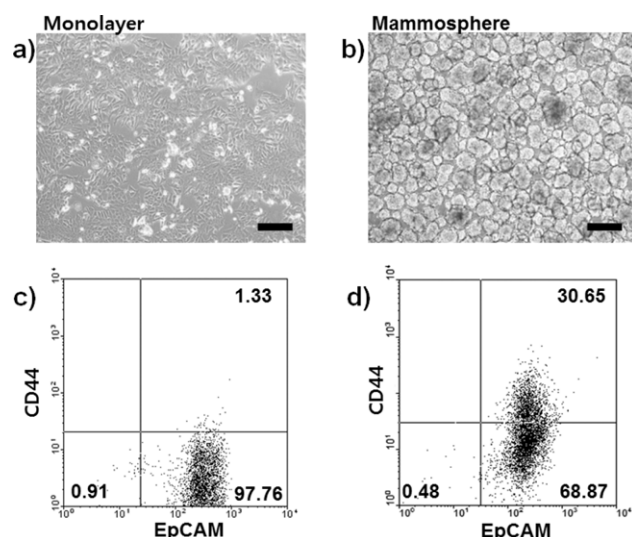


Figure 1. Microscopic images of (a) MCF7 cell monolayer and (b) MCF7 cell-derived mammospheres. Scale bars are 200 μm . Flow cytometry analyzed data for (c) MCF7 monolayer cells and (d) MCF7 cell-derived mammospheres for CD44 and EpCAM expression.

2.4. Preparation of CD44-targetable PGNRs

Polyethylene glycol-coated gold nanorods (PGNRs) were synthesized according to our previous report [10, 19]. Specifically, hetero-bi-functionalized PEG (thiol-poly(ethylene glycol)-carboxymethyl) was used as a stabilizer and cross-linker. 3-(3-dimethylaminopropyl)-carbodiimide (EDC,

2.9 μmol), *N*-hydroxysulfosuccinimide (Sulfo-NHS, 2.5 μmol), and 3 μl anti-CD44 antibody solution (Cell Signaling Technology) were added to 2 ml of the PGNR solution (259.8 μg of Au/200 μl) and reacted at 4 $^{\circ}\text{C}$ for 6 h. After centrifugation (27 000g-force for 30 min), CD44-conjugated PGNRs were dispersed in 4 ml PBS (pH 7.4). The size and morphology of CD44-conjugated PGNRs were observed using a scanning electron microscope (SEM, JSM-7001F, JEOL Ltd). Absorbance spectra for PGNR and CD44-conjugated PGNRs were evaluated using a spectrometer (Optizen 2120UV, MECASYS). The concentration of GNRs was measured using inductively coupled plasma atomic emission spectroscopy (Thermoelectron Corp.).

2.5. Binding affinity of CD44-targetable PGNRs

To determine the affinity of CD44-targetable PGNRs for MCF7 mammospheres, cells were seeded at 50 mammospheres/well in four-well tissue culture plates and then incubated with PGNRs (50; $\times 1$, 100; $\times 2$, and 150 μl ; $\times 3$, 1.0 mg Au ml^{-1}) and CD44-targetable PGNRs (50; $\times 1$, 100; $\times 2$, and 150 μl ; $\times 3$, 1.0 mg Au ml^{-1}) for 4 h at 37 $^{\circ}\text{C}$. The treated mammospheres were washed five times with PBS (pH 7.4) to eliminate unbound nanoparticles. To observe the binding affinity of the CD44-targetable GNRs with MCF7 mammospheres, light-scattering images were recorded using an inverted microscope (Olympus BX51) with a high numerical aperture dark-field condenser (U-DCW, Olympus). Immersion oil (n.d.: 1.516, Olympus) was used to balance the refractive index. Dark-field images were captured using an Olympus CCD camera.

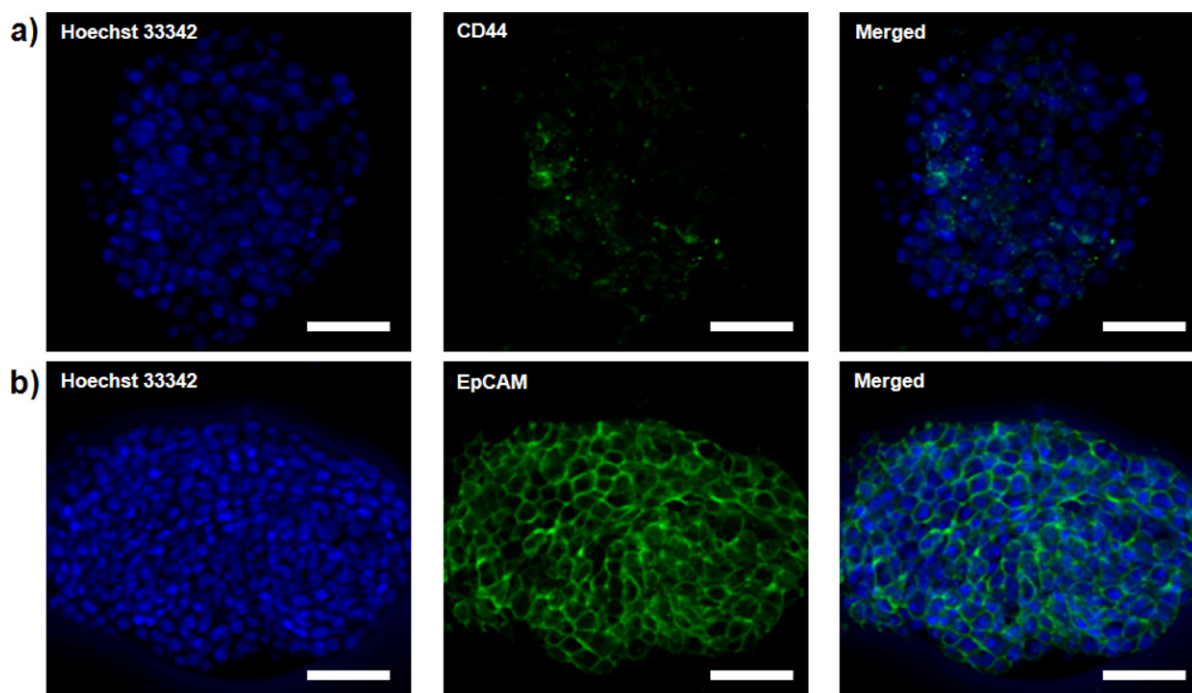


Figure 2. Confocal microscopy images of MCF7 cell mammospheres; (a) CD44 (green, FITC) and (b) EpCAM (green, FITC). Nuclei are stained blue using Hoechst 33 342. All scale bars are 20 μm .

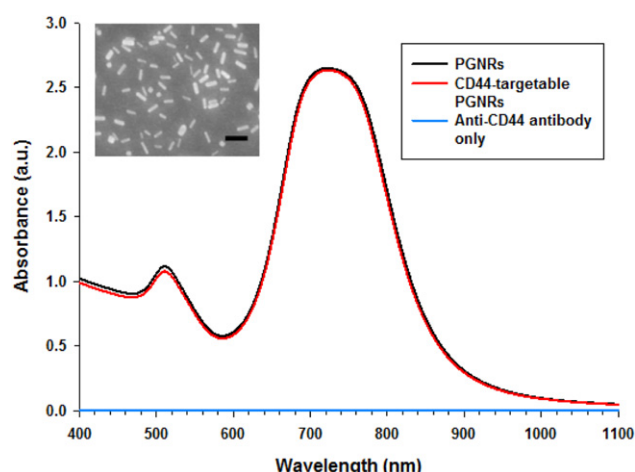


Figure 3. Absorbance spectra for PGNRs (black), anti-CD44 antibody only (blue), and CD44-targetable PGNRs (red). Inset: SEM image of PGNR. The scale bar is 100 nm.

2.6. Cytotoxicity of CD44-targetable PGNRs

The cytotoxicities of PGNRs and CD44-targetable PGNRs for MCF7 mammospheres were evaluated by a colorimetric assay, based on the cellular reduction of 3-(4,5-dimethylthiazol-2-yl)-2,5-diphenyltetrazolium bromide (MTT) (Cell Proliferation Kit I, Roche, Germany) in metabolically active cells. In a typical cell viability experiment, MCF7 mammospheres (50 spheres/well) were seeded into 96-microwell plates and incubated at 37 °C. The mammospheres were incubated with fresh medium (100 μ l) containing PGNRs (50; $\times 1$, 100; $\times 2$, and 150 μ l; $\times 3$, 1.0 mg Au ml⁻¹) or CD44-targetable PGNRs (50; $\times 1$, 100; $\times 2$, and 150 μ l; $\times 3$,

1.0 mg Au ml⁻¹) at 37 °C. 4 h after the incubation, the yellow MTT solution was treated, and the formazan crystals formed were solubilized with 10% sodium dodecyl sulfate in 0.01 M HCl. Then the absorbance of the resulting colored solution was measured at 584 nm and at 650 nm as a reference using a microplate spectrophotometer (EpochTM, BioTek, USA). Cell viability was determined from the intensity ratio of treated to non-treated control cells and shown as an average \pm standard deviation ($n = 3$).

2.7. In vitro photothermal ablation of CD44-positive subpopulations in MCF7 mammospheres

MCF7 mammospheres (50 mammospheres/well) were incubated with CD44-targetable PGNRs solution (50; $\times 1$, 100; $\times 2$, and 150 μ l; $\times 3$, 1.0 mg Au ml⁻¹) and PGNRs (50; $\times 1$, 100; $\times 2$, and 150 μ l; $\times 3$, 1.0 mg Au ml⁻¹) without CD44 antibodies at 37 °C for 4 h in four-well culture plates. Cells were rinsed with PBS (pH 7.4), and 500 μ l phenol red-free medium was added to each well. For laser irradiation experiments, cells were exposed to a NIR coherent diode laser (808 nm, 40 W cm⁻²) for 30 min to induce photothermal cell damage. The laser calibration is conducted using a laser power meter (S120C, Thorlabs) immediately below the sample stage before the laser irradiation. The beam diameter is measured using a general ruler through a guide beam that was transmitted to thin lens cleaning tissue. For the live/dead assay, 1 μ M ethidium bromide (EtBr, Sigma) and 5 μ M calcein AM (Molecular Probes) solution were added and incubated for 30 min at 37 °C. After the washing with PBS (pH 7.4), we evaluated cellular viability by fluorescence microscopy (Olympus BX51) at 2, 18, and 36 h after NIR laser irradiation. Cell populations expressing

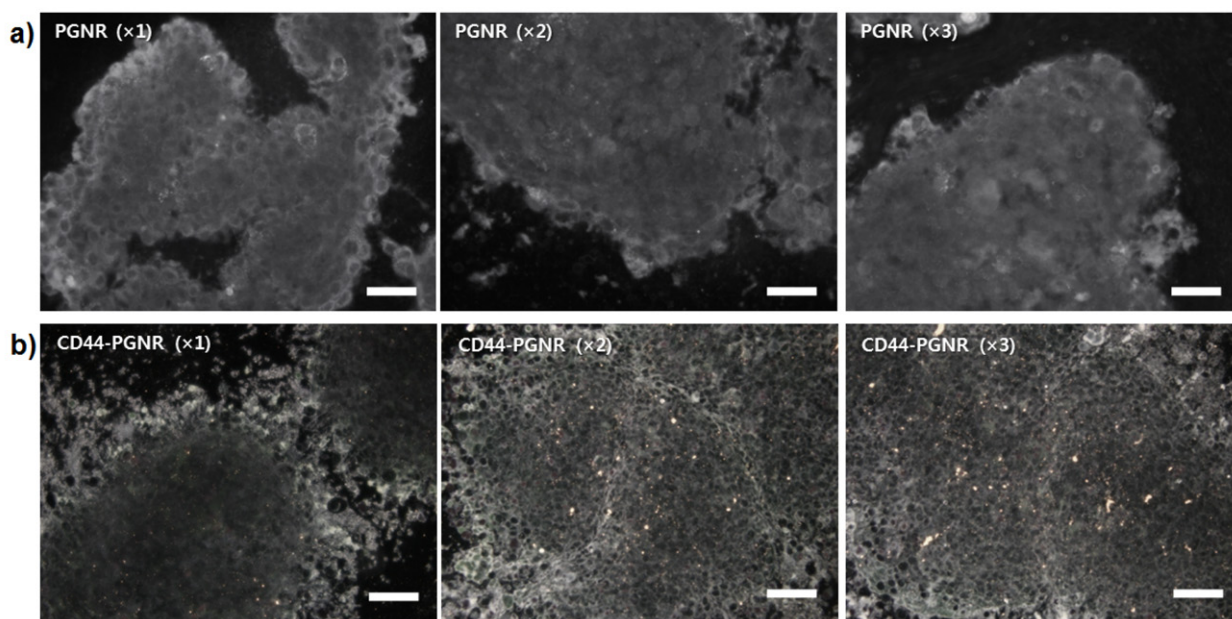


Figure 4. Dark-field microscopy images of MCF7 mammospheres treated with (a) non-labeled PGNRs ($\times 1$, $\times 2$, and $\times 3$) and (b) CD44-targetable PGNRs ($\times 1$, $\times 2$, and $\times 3$), respectively. All scale bars are 10 μ m.

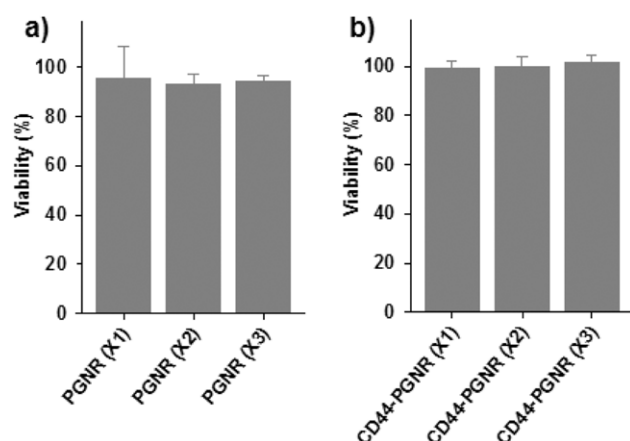


Figure 5. Viability of MCF7 mammospheres treated with PGNR ($\times 1$, $\times 2$, and $\times 3$) or CD44-targetable PGNRs ($\times 1$, $\times 2$, and $\times 3$) measured by MTT assay.

CD44 were assessed by flow cytometry for photothermally damaged mammospheres at 2, 18, and 36 h after NIR laser irradiation. Morphological changes for MCF7 mammospheres after photothermal ablation were observed by microscopy at 2, 18, and 36 h after NIR laser irradiation.

3. Results and discussion

Self-renewal and tumorigenic abilities of MCF7 breast cancer cell subpopulations emerge when these cells are cultured in mammosphere-forming conditions [18]. These mammospheres become heterogeneous and contain stem cell-like subpopulations that are characterized by CD44 expression [6]. Thus, we prepared MCF7 mammospheres as a model system for increasing tumorigenic CD44-positive populations for experimentation. Parental MCF7 cell monolayers (figure 1(a)) were trypsinized, washed, and grown in ultra-low attachment-coated culture plates. After seven days under mammosphere culture conditions, acinus-like

three-dimensional structured MCF7 mammospheres were observed by phase-contrast microscopy. Mammospheres were between 50 and 100 μm in diameter (figure 1(b)).

CD44 and EpCAM expression levels of MCF7 monolayers and mammospheres were evaluated by flow cytometry. Formation of MCF7 mammospheres increased the percentage of CD44-positive cells from 1.33% in parental MCF7 monolayer cells to 30.65% of mammosphere cells (figures 1(c) and (d)). Moreover, immunofluorescence microscopic images for MCF7 mammospheres were obtained (figure 2). Vivid green fluorescence spots for MCF7 mammospheres represented MCF7 cancer cells that upregulated CD44 during the mammosphere formation (figure 2(a)). In both monolayer and mammosphere MCF7 cells, EpCAM expression levels were high and not significantly different from one another (figures 1(c), (d) and 2(b)).

To fabricate a smart photothermal probe, we synthesized GNRs based on a seed-mediated growth process. After the synthesis of PGNRs, the size and morphology were analyzed using SEM (figure 3, inset) and we determined that the longitudinal length of the GNR is 38 ± 3.5 nm and the transverse length of the GNRs is 10 ± 1.1 nm ($n = 100$). The aspect ratio of the GNRs is, therefore, calculated as about 4 using the above mentioned values. As we previously reported [10], rod-like plasmonic nanoparticles with high NIR absorbance were prepared and the absorbance spectrum is depicted in figure 3 (black line). We initially used the ligand CTAB, but found it to be cytotoxic due to high cationic property. Thus, CTAB was substituted with polyethylene glycol as an inert linker molecule. For the attachment of anti-CD44 antibodies to GNRs, we used the hetero-functional carboxyl PEG and thiol PEG molecules. Anti-CD44 antibody was conjugated to PGNRs using EDC and Sulfo-NHS as linking agents in PBS (pH 7.4). After immobilization of the targeting antibody to PGNRs, the absorbance spectrum was examined and the characteristic peak was similar to that for bare PGNRs (figure 3, red line). As expected, any characteristic peaks for bare anti-CD44 antibody were not

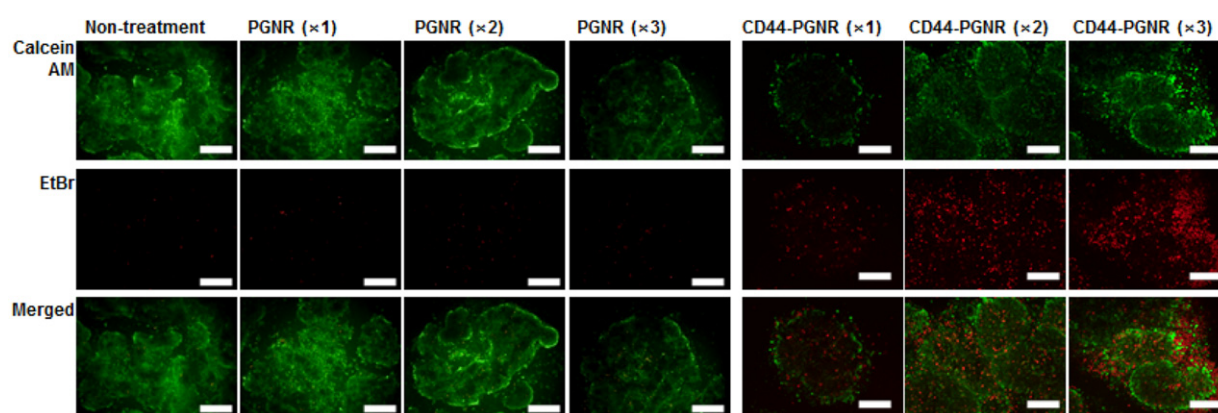


Figure 6. Fluorescence microscopy images of MCF7 cell mammospheres after treatment with either unlabeled PGNRs ($\times 1$, $\times 2$, and $\times 3$) or CD44-targetable PGNRs ($\times 1$, $\times 2$, and $\times 3$ concentrations), followed by NIR laser irradiation (808 nm, 40 W cm^{-2}). Green fluorescence indicates live cell staining by calcein AM. Red fluorescence indicates dead cell nuclei stained by ethidium bromide. All scale bars are 50 μm .

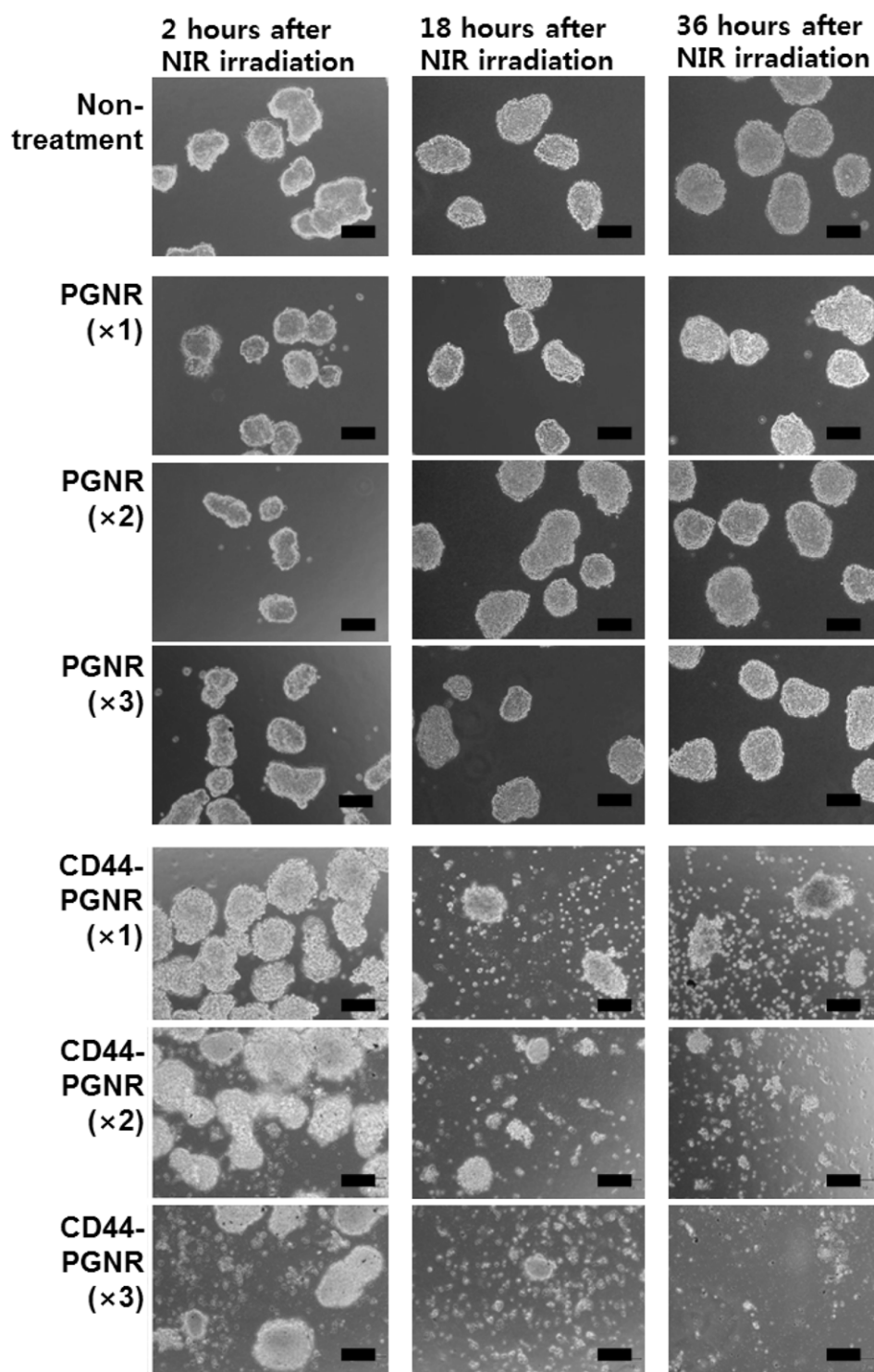


Figure 7. Phase-contrast microscopy images of MCF7 cell mammospheres treated with PGNRs ($\times 1$, $\times 2$, and $\times 3$) or CD44-targetable PGNRs ($\times 1$, $\times 2$, and $\times 3$ concentrations) at various time points (2, 18, and 36 h) after NIR laser irradiation (808 nm, 40 W cm^{-2}). All scale bars are $100 \mu\text{m}$.

observed due to the low concentration (figure 3, blue line) and the amounts of antibody conjugated to PGNR did not affect the result for the absorbance for CD44-targetable PGNRs (figure 3, red line). Thus, the antibody conjugation did not change the optical properties for CD44-targetable PGNRs as a photothermal agent using an NIR laser.

To investigate the targeting ability of anti-CD44 antibody-modified PGNRs, either PGNR alone (without conjugated anti-CD44 antibody; negative control) or CD44-targetable PGNRs were incubated with MCF7 mammospheres. It was found by dark-field microscopy, as shown in figure 4, that bright yellow spots due to light scattering by

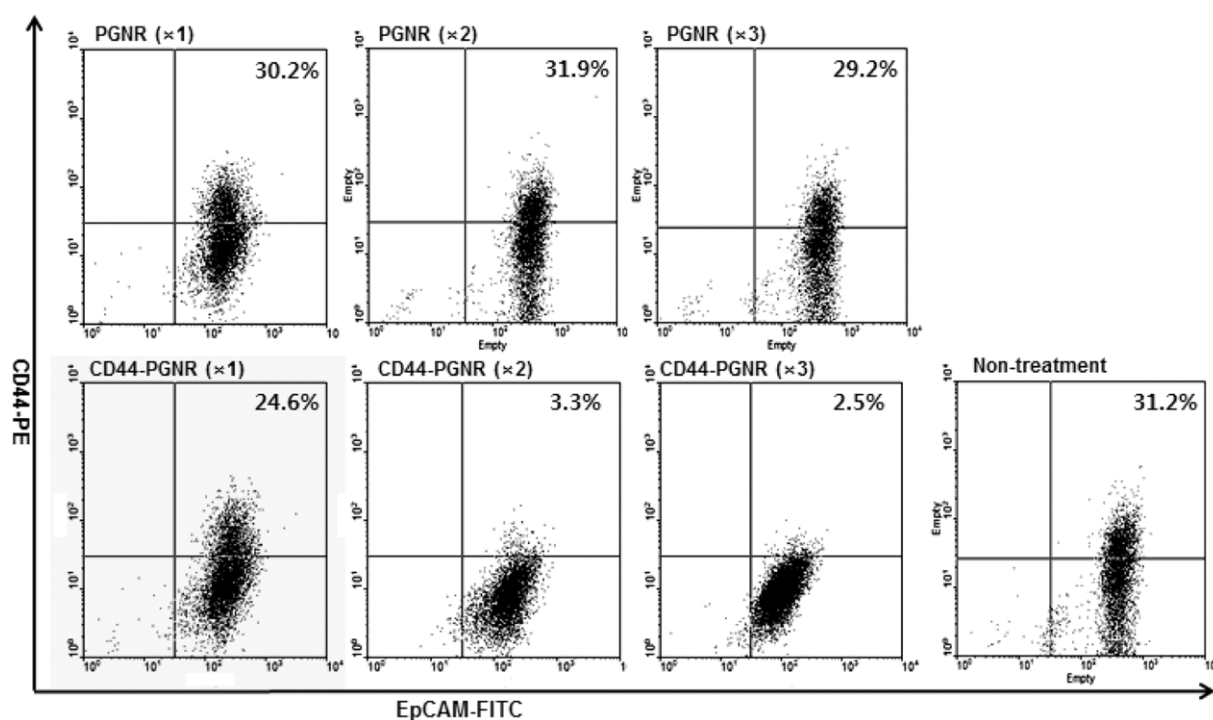


Figure 8. Flow cytometric analysis data (stained with CD44-PE and EpCAM-FITC) of MCF7 cell mammospheres treated with either unlabeled PGNRs ($\times 1$, $\times 2$, and $\times 3$) or CD44-targetable PGNRs ($\times 1$, $\times 2$, and $\times 3$ concentrations) 36 h after NIR laser irradiation (808 nm, 40 W cm^{-2}).

GNRs that were bound to mammospheres gradually increased in number as CD44-targetable PGNR concentrations were raised from $\times 1$ to $\times 3$. However, bare PGNRs ($\times 1$ to $\times 3$, without anti-CD44 antibody conjugation) were not attached to MCF7 mammospheres due to the absence of the targeting moiety, anti-CD44 antibody. These results demonstrate that the CD44-targetable PGNRs can be selectively delivered to CD44-positive MCF7 cell populations in mammospheres, and facilitate localized cell ablation by directed NIR laser irradiation. Furthermore, the treatment of PGNR or CD44-targetable PGNRs for MCF7 mammospheres did not induce the severe cytotoxic effect without NIR laser irradiation (figure 5).

As previously described, CD44 may be one of the most important biomarkers involved in cancer relapse and metastasis. Furthermore, CD44 expression is, directly or indirectly, regulated by the β -catenin/Tcf-4 signal pathway [20, 21], suggesting a role for CD44 in tumorigenesis. Thus, the disruption of CD44 function or ablation of CD44-expressed cancer cells can be a kernel strategy for effective cancer therapy in metastatic mammary carcinoma [22, 23]. To assess the photothermal ablation efficacy against CD44-generated mammospheres, MCF7 mammospheres were treated with CD44-targetable PGNR and then NIR laser irradiated (40 W cm^{-2}). At 30 min after laser irradiation, a live–dead assay was conducted using calcein AM and ethidium bromide. Control MCF7 mammospheres treated with unlabeled PGNRs ($\times 1$, $\times 2$, and $\times 3$, $1.0 \text{ mg Au ml}^{-1}$) did not exhibit red fluorescence, which would be indicative of cell killing and ethidium bromide reacting with cellular nucleic acids (figure 6). Thus, unlabeled PGNR did not attach to MCF7 cells. However, CD44-targetable PGNRs caused effective

photothermal ablation of CD44-expressing MCF7 cancer cells. At a low concentration of anti-CD44 antibody-linked PGNRs ($\times 1$), red fluorescence spots were observed in the mammospheres. As we increased the CD44-targetable PGNR concentration ($\times 2$ and $\times 3$), dead cell populations were increased. At high concentration of the photothermal probes, the dead cells spread out from the mammospheres. To investigate longer-term effects of photothermal therapy, we incubated the treated and irradiated mammospheres for up to 36 h. Unlabeled PGNR-treated MCF7 mammospheres showed no change in viability and morphology after 36 h incubation (figure 7). However, the photothermally damaged mammospheres that had been selectively targeted with anti-CD44-linked PGNRs and then NIR laser irradiated underwent further disruption over time. Flow cytometric analysis (figure 8) demonstrated a clear selective killing effect of the CD44-positive MCF7 cell fraction from mammospheres. The percentages of CD44-positive MCF7 tumorigenic cells were 31.2% in non-treated cases, and 30.2% ($\times 1$), 31.9% ($\times 2$), 29.2% ($\times 3$), in unlabeled PGNR-treated mammospheres. These values dramatically dropped after CD44-targetable PGNR photothermal ablation, with only 3.3% and 2.5% of cells in CD44-PGNR-treated mammospheres remaining after respectively $2\times$ and $3\times$ CD44-PGNR treatments. However, CD44-targeted MCF7 cell ablation had no effect on EpCAM-expressing cell numbers in mammospheres, versus controls. These results demonstrate the highly selective and effective photothermal ablation of a specific population of CD44-positive cancer cells, using targeted PGNRs in concert with NIR laser irradiation.

4. Conclusion

We developed a model system for the selective photothermal ablation of specific cancer cell subpopulations in cellularly heterogeneous tumor-like three-dimensional mammospheres. CD44-positive populations, reported to exhibit tumorigenic and self-renewal potentials, were generated by engineering MCF7 cells into mammospheres using defined culture conditions. The proportion of CD44-positive cell populations in MCF7 mammospheres was approximately tenfold increased as compared to MCF7 cell monolayers, as confirmed by flow cytometry and immunofluorescence microscopy. To investigate the therapeutic potential of molecularly targeted photothermal cell ablation, plasmonic gold nanoparticles (GNRs) were synthesized and coated, using a PEG linker, to a targeting moiety (anti-CD44 antibody). This allowed the selective targeted delivery of GNRs to CD44-expressed cancer cells. The prepared CD44-specific GNRs exhibited strong NIR light absorption that enabled photothermal ablation of target cells by NIR laser irradiation. We demonstrated the utility of this system for selectively and effectively destroying tumorigenic CD44-expressing MCF7 cells in mammospheres, while surrounding cells were undisturbed. Thus, our therapeutic system for biomarker-specific cell ablation using a photo-induced heat-generating nanoplatform is a potential strategy for effectively ablating stem cell-like cancer cell subpopulations from the tumor burden, to effectively treat cancer.

Acknowledgment

This research was supported by the National Research Foundation of Korea (NRF) funded by the Ministry of Education, Science and Technology (2010-0023202 and 2010-0019923).

References

- [1] Clarke M F, Dick J E, Dirks P B, Eaves C J, Jamieson C H M, Jones D L, Visvader J, Weissman I L and Wahl G M 2006 Cancer stem cells—perspectives on current status and future directions: AACR workshop on cancer stem cells *Cancer Res.* **66** 9339–944
- [2] Stingl J and Caldas C 2007 Molecular heterogeneity of breast carcinomas and the cancer stem cell hypothesis *Nature Rev. Cancer* **7** 791–9
- [3] Takahashi R U, Takeshita F, Fujiwara T, Ono M and Ochiya T 2011 Cancer stem cells in breast cancer *Cancers* **3** 1311–28
- [4] Nguyen L V, Vanner R, Dirks P and Eaves C J 2012 Cancer stem cells: an evolving concept *Nature Rev. Cancer* **12** 133–43
- [5] Li F, Tiede B, Massagué J and Kang Y 2007 Beyond tumorigenesis: cancer stem cells in metastasis *Cell Res.* **17** 3–14
- [6] Al-Hajj M, Wicha M, Benito-Hernandez A, Morrison S and Clarke M 2003 Prospective identification of tumorigenic breast cancer cells *Proc. Natl Acad. Sci. USA* **100** 3983–8
- [7] Ailles L E and Weissman I L 2007 Cancer stem cells in solid tumors *Curr. Opin. Biotechnol.* **18** 460–6
- [8] Visvader J E and Lindeman G J 2008 Cancer stem cells in solid tumours: accumulating evidence and unresolved questions *Nature Rev. Cancer* **8** 755–68
- [9] Yang J, Lee J, Kang J, Oh S J, Ko H J, Son J H, Lee K, Suh J S, Huh Y M and Haam S 2009 Smart drug-loaded polymer gold nanoshells for systemic and localized therapy of human epithelial cancer *Adv. Mater.* **21** 4339–42
- [10] Choi J, Yang J, Bang D, Park J, Suh J S, Huh Y M and Haam S 2012 Targetable gold nanorods for epithelial cancer therapy guided by near-IR absorption imaging *Small* **8** 746–53
- [11] Huang X, El-Sayed I H, Qian W and El-Sayed M A 2006 Cancer cell imaging and photothermal therapy in the near-infrared region by using gold nanorods *J. Am. Chem. Soc.* **128** 2115–20
- [12] Choi J, Yang J, Jang E, Suh J S, Huh Y M, Lee K and Haam S 2011 Gold nanostructures as photothermal therapy agent for cancer *Anticancer Agents Med. Chem.* **11** 953–64
- [13] Jain P K, Huang X, El-Sayed I H and El-Sayed M A 2008 Noble metals on the nanoscale: optical and photothermal properties and some applications in imaging, sensing, biology, and medicine *Acc. Chem. Res.* **41** 1578–86
- [14] Alkilany A M, Thompson L B, Boulos S P, Sisco P N and Murphy C J 2012 Gold nanorods: their potential for photothermal therapeutics and drug delivery, tempered by the complexity of their biological interactions *Adv. Drug Deliv. Rev.* **64** 190–9
- [15] Sheridan C, Kishimoto H, Fuchs R, Mehrotra S, Bhat-Nakshatri P, Turner C, Goulet R, Badve S and Nakshatri H 2006 CD44+/CD24–breast cancer cells exhibit enhanced invasive properties: an early step necessary for metastasis *Breast Cancer Res.* **8** R59
- [16] Ponta H, Sherman L and Herrlich P A 2003 CD44: from adhesion molecules to signalling regulators *Nature Rev. Mol. Cell Biol.* **4** 33–45
- [17] Ao A, Morrison B J, Wang H, López J A, Reynolds B A and Lu J 2011 Response of estrogen receptor-positive breast cancer tumorspheres to antiestrogen treatments *PLoS One* **6** e18810
- [18] Xie G et al 2012 Mammosphere cells from high-passage MCF7 cell line show variable loss of tumorigenicity and radioresistance *Cancer Lett.* **316** 53–61
- [19] Choi J, Yang J, Park J, Kim E, Suh J S, Huh Y M and Haam S 2011 Specific near-IR absorption imaging of glioblastomas using integrin-targeting gold nanorods *Adv. Funct. Mater.* **21** 1082–8
- [20] Liu B Y, McDermott S P, Khwaja S S and Alexander C M 2004 The transforming activity of Wnt effectors correlates with their ability to induce the accumulation of mammary progenitor cells *Proc. Natl Acad. Sci. USA* **101** 4158–63
- [21] Li Y et al 2003 Evidence that transgenes encoding components of the Wnt signaling pathway preferentially induce mammary cancers from progenitor cells *Proc. Natl Acad. Sci. USA* **100** 15853–8
- [22] Yu Q, Toole B P and Stamenkovic I 1997 Induction of apoptosis of metastatic mammary carcinoma cells *in vivo* by disruption of tumor cell surface CD44 function *J. Exp. Med.* **186** 1985–96
- [23] Zuckerman V, Wolynec K, Sionov R V, Haupt S and Haupt Y 2009 Tumour suppression by p53: the importance of apoptosis and cellular senescence *J. Pathol.* **219** 3–15